ANALYTICAL THEORY OF FEEDBACK-CONTROLLED PERIODIC STATES IN PHOTOREFRACTIVE CRYSTALS[1]

E. V. PODIVILOV, B. I. STURMAN, M. GORKOUNOV[1]

International Institute for Nonlinear Studies
(1, Koptyug Ave., Novosibirsk 630090, Russia),

[1]**University of Osnabrück**
(Department of Physics, University of Osnabrück, D-49069 Osnabrück, Germany;
Permanent address: Institute of Crystallography of RAS, 59, Lenin Ave., Moscow, Russia)

UDC 535.215

Employment of certain feedbacks in photorefractive optical schemes allows one to realize periodic states (attractors) with ultimately high or low diffraction efficiency. This strongly nonlinear phenomenon has been studied experimentally and numerically. We propose and develop an analytical method for the analysis of periodic states by making use of the symmetry properties of the coupled-wave equations and the high-speed response of the feedback loop. Various periodic states are described in detail. This includes the regions of existence, the period and amplitude of oscillations of measurable output parameters, and the shape of strong non-periodic phase modulation of the input beams.

Introduction

Beam-coupling phenomena in photorefractive (PR) media have been the subject of many experimental and theoretical studies during the last two decades (see, e.g., [1–7]). This is caused by the diversity and strength of nonlinear photorefractive effects and by their great application potential.

Controlling nonlinear optical processes in PR crystals by electronic feedbacks has attracted much attention during the last years [8–13]. A typical experimental setup is sketched in Fig. 1. The phase of the input signal beam, φ_s, is coupled in a certain way (see below for details) with its output intensity. This results in strong changes of the apparent characteristics of two-wave coupling.

Originally, the feedback was introduced to suppress the influence of phase fluctuations at the input, i.e., to stabilize a photorefractive setup. Experiment has shown, however, that the effect of the feedback loop is much stronger than the expected one. In particular, the recorded dynamic index grating showed an almost 100% diffraction efficiency and the energy exchange between the pump beams was significantly suppressed [8–10]. First attempts to explain the observed features, by assuming that the recorded grating is spatially uniform, were not successful. They included, however, the fruitful idea that the feedback maintains a $\pm\pi/2$ phase shift between the diffracted and transmitted components of the signal beam.

In [11], the coupled-wave equations for light amplitudes were supplemented by nonlocal boundary conditions relevant to the $\pm\pi/2$ — feedback and direct numerical simulations were performed. It was shown that the ideal $\pm\pi/2$ — feedback really maximizes or minimizes (depending on the feedback sign) the diffraction efficiency within a finite time. After this efficiency has reached an ultimate value, the ideal feedback condition becomes unapplicable, since one of the signal beam components (diffracted or transmitted) turns to zero. Thus, the ideal-feedback model is incapable of describing the permanent operation feedback setup observed experimentally.

It was found later [12, 13] that inertia of the electronic feedback loop is the key element for the permanent operation of the whole nonlinear system. Numerical simulations with inertial feedback conditions have shown that the system arrives at a periodic state where the input phase $\varphi_s(t)$ experiences strong and fast periodic oscillations superimposed on a constant drift. Furthermore, a variation of the input intensity ratio or/and the crystal thickness causes transitions between different periodic states. Special experiments with $LiNbO_3$ crystals have confirmed the presence of various periodic states [12].

It should be emphasized that the nonlinear system under study is far from trivial. To the best of our knowledge, it has no analogs in the domain of nonlinear optics because the nonlinear evolution of wave amplitudes is governed by a nonlocal and nonlinear feedback. The known examples of direct numerical calculations cannot exhaust the problem and make its theoretical study even more challenging.

[1]This article is dedicated to Professor Marat Soskin on the occasion of his 75th birthday.

Below, we propose and develop an analytical method to describe the feedback-controlled nonlinear evolution. The main idea is to apply the procedure of averaging over the fast phase oscillations [14]. This method exploits the only small parameter of theory — the ratio of the feedback loop response time to the response time of the photorefractive nonlinearity. Certain symmetry properties of the coupled-wave equations are also highly important for our considerations. Furthermore, we restrict ourself to the local PR response – the simplest and most important case for practice. This limitation is not crucial, the results obtained can be further generalized for other types of the photorefractive response.

1. Basic Relations

A. Two-wave Coupling Equations

Initial coupled-wave equations for the amplitudes of the signal and reference waves, S and R, and the grating amplitude E, see also Fig. 1, can be presented in the following dimensionless form:

$$R_x = iES, \tag{1}$$

$$S_x = iE^*R, \tag{2}$$

$$E_t + E = RS^*. \tag{3}$$

The subscripts x and t denote taking the partial derivatives with respect to the coordinate and time, respectively. The coordinate x is normalized to the characteristic length of wave interaction, which is independent of the light intensity, whereas t is normalized to the PR response time which is inversely proportional to the total light intensity.

Equations (1) and (2) follow from Maxwell's equations and describe Bragg diffraction of R- and S-waves on the index grating, and the total light intensity does not depend on x. Since the input ($x = 0$) intensities are expected to be time independent, the total intensity remains constant. This allows one to normalize the amplitudes R and S in such a way that $|R(x,t)|^2 + |S(x,t)|^2 = 1$.

Equation (3) describes the grating formation under the action of light; it models charge-transport properties properties of the medium [3,11]. The absolute value of the RS^* product is nothing else than the half-contrast of the interference pattern. According to (3), the steady-state grating amplitude is $E = RS^*$. The corresponding space-charge field profile is not shifted with respect to the light interference pattern so that the PR response is local within our considerations.

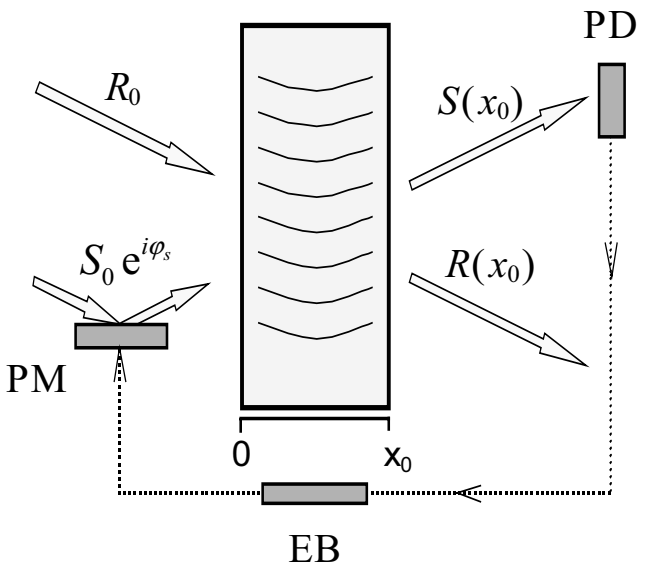

Fig. 1. Schematic presentation of feedback-controlled two-beam coupling: PM is a piezo-mirror, PD is a photodetector, and EB is an electronic block. The parallel bent lines show the grating fringes

B. Fundamental Amplitudes

The spatial dependences $R(x)$ and $S(x)$ are determined by the input values $R(0)$, $S(0)$ (the readout conditions) and the grating profile $E(x)$; it is implied that these quantities depend generally on the time t. It is important to realize that the same grating can be readout in different ways if the input amplitudes are changing rapidly. This feature is clearly seen from the structure of Eqs. (1) — (3): Equation (3) ensures that the profile $E(x)$ remains almost unchanged during the time period $\delta t \ll 1$ when we analyze the changes of the output characteristics during a fast modulation of the input amplitudes $R(0,t)$ and $S(0,t)$ with the help of Eqs. (1), (2).

The set of differential equations (1), (2) is linear and homogeneous with respect to R and S. Its general solution, as known from basic mathematics, can be presented as a linear combination of two independent particular solutions.

As the first particular solution, we choose the pair of fundamental amplitudes $R_F(x)$, $S_F(x)$ that obey Eqs. (1), (2) and meet the boundary conditions $R_F(0) = 1$, $S_F(0) = 0$; physically, this solution describes the readout of a grating by the R-beam of a unit amplitude.

Since $E = E(x,t)$, the fundamental amplitudes are generally functions of t.

It is easy to check furthermore that the pair $R = -S_F^*(x)$, $S = R_F^*(x)$ is also a particular solution of set (1), (2) which is linearly independent of the first one. This second solution describes the readout of the same grating by the S-beam of a unit amplitude. The mentioned link between two different solutions is, indeed, a consequence of symmetry properties of the readout equations. Owing to this symmetry, the pair of fundamental amplitudes $R_F(x,t)$, $S_F(x,t)$ fully describes the diffraction properties of the grating.

The general solution $R(x,t)$, $S(x,t)$ with the boundary conditions $R_0(t)$, $S_0(t)$ can be presented in the form

$$R(x,t) = R_F(x,t)R_0(t) - S_F^*(x,t)S_0(t),$$

$$S(x,t) = S_F(x,t)R_0(t) + R_F^*(x,t)S_0(t). \qquad (4)$$

These relationships allow us to express algebraically the fundamental amplitudes R_F, S_F by the recording amplitudes $R(x,t)$, $S(x,t)$. It is useful to keep in mind during this procedure that $|R_F(x,t)|^2 + |S_F(x,t)|^2 = 1$.

The formulation of feedback conditions requires a separation of the amplitudes R and S into the transmitted (T) and diffracted (D) components. Equations (4) serve best to this purpose. As seen from them and Fig. 1, the product R_0R_F describes the transmitted component of the R-beam, whereas the combination $-S_0S_F^*$ characterizes the diffracted part of the S-beam. Similarly, the products S_FR_0 and $R_F^*S_0$ are the D- and T-components of the amplitude $S(x,t)$.

Lastly, we mention that the parameter $\eta = |S_F(x_0,t)|^2 \equiv 1 - |R_F(x_0,t)|^2$, where x_0 is the crystal thickness, is nothing else than the diffraction efficiency of the grating. It can be measured by a short-time blocking of one of the input recording beams (R or S).

C. Feedback Conditions

In what follows we assume that the amplitude of the input R-beam is constant, $R(0,t) = R_0 = \text{const}$, while the amplitude of the input S-beam is phase modulated, $S(0,t) = S_0\exp(i\varphi_s)$, where $S_0 = \text{const}$ and $\varphi_s = \varphi_s(t)$. The variable external parameters are the crystal thickness x_0 and the input intensity ratio $r_0 = |R_0|^2/|S_0|^2$.

The phase difference between the diffracted, $S_F(x_0)R_0$, and transmitted, $R_F^*(x_0)S_0\exp(i\varphi_s)$, components of the output S-beam is

$$\Phi_s = \arg\left[R_0S_0^*R_F(x_0)S_F(x_0)\exp(-i\varphi_s)\right]. \qquad (5)$$

The equalities $\Phi_s = \pm\pi/2$ are known as the ideal feedback conditions. They can be satisfied by a certain choice of the input phase φ_s. Since the fundamental amplitudes are expressed by R and S, the feedback imposes a nonlinear coupling between φ_s and output amplitudes of the recording beams. Obviously, the value Φ_s is defined only for $\eta \neq 0, 1$, i.e., for nonzero $|S_F(x_0)R_F(x_0)| \equiv \sqrt{\eta(1-\eta)}$.

Experimentally, the feedback is implemented by introducing an auxiliary oscillating component into the input phase of the S-beam, $\delta\varphi_s = \psi_d\sin(\omega t)$ where $\psi_d \ll 1$, $\omega \gg 1$. It does not affect the recording and serves as a marker of the T-component of the S-beam. Interference of the D and T components gives rise to oscillations of the output intensity $|S(x_0,t)|^2$ on the double frequency 2ω; the corresponding oscillation amplitude is $I_{2\omega} = |R_0S_0|\sqrt{\eta(1-\eta)}\,\psi_d^2\cos(\Phi_s)/2$. Using the intensity oscillations as an error signal in an electronic feedback loop, it is possible to adjust the phase difference Φ_s to $\pm\pi/2$ unless $\eta(1-\eta) = 0$.

It has been found experimentally [8] that the diffraction efficiency η approaches unity and remains then very close to this value in the presence of the $+\pi/2$ feedback. Changing the feedback sign leads to a state with $\eta \simeq 0$ (transparent grating). Numerical simulations have shown that the ideal feedback conditions, $\Phi_s \pm \pi/2$, describe perfectly well the initial stage of evolution (when η is approaching 1 or 0) but fail to describe the permanent operation of the feedback system [11]. The reason is that the phase difference Φ between the D- and T-components of the signal beam loses its meaning when one of these components turns to zero.

It was proved then that the inertia of a feedback loop is responsible for the permanent operation of the whole system [12]. Correspondingly, the ideal feedback conditions $\Phi_s \pm \pi/2$ have to be replaced by the dynamic feedback equation

$$\dot{\varphi_s} = \mp\, t_f^{-1}\,|R_0S_0|\,\sqrt{\eta(1-\eta)}\,\cos(\Phi_s), \qquad (6)$$

where $t_f \ll 1$ is the feedback loop reaction time and the dot denotes taking the ordinary derivative with respect to the time t. The meaning of this inertial feedback condition can be commented as follows: Until the factor before $\cos(\Phi_s)$ is large as compared to unity, the input phase φ_s relaxes quickly to a value that provides the equality $\Phi_s \simeq \pm\pi/2$, i.e., fulfilment of the ideal feedback condition. When the product $\eta(1-\eta)$ approaches zero, the feedback inertia becomes important and Φ_s deviates strongly from the ideal $\pm\pi/2$ values.

Numerical simulations with the use of Eq. (6) have shown [12,13] that the diffraction efficiency approaches quickly an ultimate value (1 or 0) and oscillates then in its close vicinity with a period of $T < 1$, while the phase φ_s experiences strong T-periodic oscillations superimposed on the linear drift,

$$\varphi_s = \Omega t + \varphi_p(t). \tag{7}$$

The part of Ω which is multiple of $2\pi/T$ can be included into the fast periodic function $\exp(i\varphi_p)$. In such a way, the inertial feedbacks lead, in accordance with experiment, to certain periodic states (attractors) instead of steady states familiar for feedback-free photorefractive systems [1,3].

By varying the external parameters x_0 and r_0, one can see the quantitative (or even qualitative) changes of the actual periodic state. These include gradual (or even sudden) changes of the detuning Ω, of the period T, and of the shape of $\varphi_p(t)$. These features have been detected in special experiments [12]. The dimensionless response time of the feedback loop, t_f, was evaluated as $\sim 10^{-3}$.

2. Analytical Approach

The presence of fast, with period $T \ll 1$, oscillations of the amplitudes enables us to use an analytical perturbational method to solve the basic equations. This method employs an averaging procedure [14]. The main steps to be undertaken are as follows: All amplitudes are separated into slow (averaged) and fast components. The averaged basic equations provide explicit expressions for slow amplitudes; these expressions include an integral parameter characterizing the influence of fast phase modulation. The periodic states can be obtained by solving ordinary differential equations for the fast amplitudes.

A. Averaged Amplitudes

In accordance with (7), we represent the fundamental amplitudes in the form

$$R_F(x,t) = \bar{R}_F(x) + \tilde{R}_F(x,t), \tag{8}$$

$$S_F(x,t) = \exp(i\Omega t)\,[\bar{S}_F(x) + \tilde{S}_F(x,t)], \tag{9}$$

$$E(x,t) = \exp(-i\Omega t)\,[\bar{E}(x) + \tilde{E}(x,t)]. \tag{10}$$

The averaged amplitudes $\bar{R}_F$, $\bar{S}_F$, $\bar{E}$ are time independent while the components $\tilde{E}$, $\tilde{R}_F$, $\tilde{S}_F$ are fast T-periodic functions of time. The same representation is valid for the recording amplitudes R and S. The frequency detuning is treated as a characteristic parameter of the averaged equations, $|\Omega| \lesssim 1$.

Owing to inertia of the PR response, the fast component of the grating amplitude is small, $\tilde{E} \ll \bar{E}$. Since the fundamental amplitudes R_F and S_F characterize instantaneous diffraction properties of the grating, this is valid for them also, $\tilde{R}_F \ll \bar{R}_F$, $\tilde{S}_F \ll \bar{S}_F$. At the same time, the fast components of the recording amplitudes, $\tilde{R}$ and $\tilde{S}$, are not small as compared to $\bar{R}$ and $\bar{S}$. Moreover, they contribute significantly to $\bar{E}$ [14].

Within the first order of our perturbation theory we neglect the fast components of R_F and S_F and obtain the averaged grating amplitude, using Eq. (3), as

$$\bar{E} = (1 - i\Omega)^{-1}\left[W_0 \bar{R}_F \bar{S}_F^* + \varepsilon\,|R_0 S_0|\,(\bar{R}_F^2 - \bar{S}_F^{*2})\right], \tag{11}$$

where $W_0 = |R_0|^2 - |S_0|^2 \equiv (r_0 - 1)/(r_0 + 1)$ is the normalized difference of the input intensities and $\varepsilon = \langle \exp(i\varphi_p(t)) \rangle$ is the average over a period of T. Since the phase $\varphi_p(t)$ is defined up to a constant, we choose $\arg(\varepsilon)$ to be zero for convenience. Then the parameter ε is real; it ranges from 0 to 1. The case $\varepsilon = 0$ corresponds to the strongest impact of the phase modulation. In the case of $\varepsilon = 1$, the modulation is absent.

Ordinary differential equations for $\bar{R}_F$ and $\bar{S}_F$ have the form of Eqs. (1), (2) with E being replaced by $\bar{E}$. The latter, as we already know, is a quadratic form of $\bar{R}_F$ and $\bar{S}_F^*$. The final result of calculations is as follows:

$$\bar{R}_F = [Q_-^2\,\exp(-\gamma x/2) + Q_+^2\,\exp(\gamma x/2)]\times$$

$$\times [Q_-^2\,\exp(-\gamma' x) + Q_+^2\,\exp(\gamma' x)]^{(i-\Omega)/2\Omega}, \tag{12}$$

$$\bar{S}_F^* = 2Q_+Q_-\,\mathrm{sh}(\gamma x/2)\,[Q_+^2\,\exp(\gamma' x) +$$

$$Q_-^2\,\exp(-\gamma' x)]^{(i-\Omega)/2\Omega}, \tag{13}$$

where

$$Q_\pm = \frac{1}{\sqrt{2}}\left(1 \mp \frac{W_0}{g}\right)^{1/2}, \tag{14}$$

$$\gamma = g(i + \Omega)^{-1}, \tag{15}$$

and

$$g = \sqrt{W_0^2 + \varepsilon^2(1 - W_0^2)}. \tag{16}$$

Obviously, we have $g \geq |W_0|$. With no phase modulation ($g = 1$), the above relations describe the conventional two-beam coupling in the presence of frequency detuning Ω.

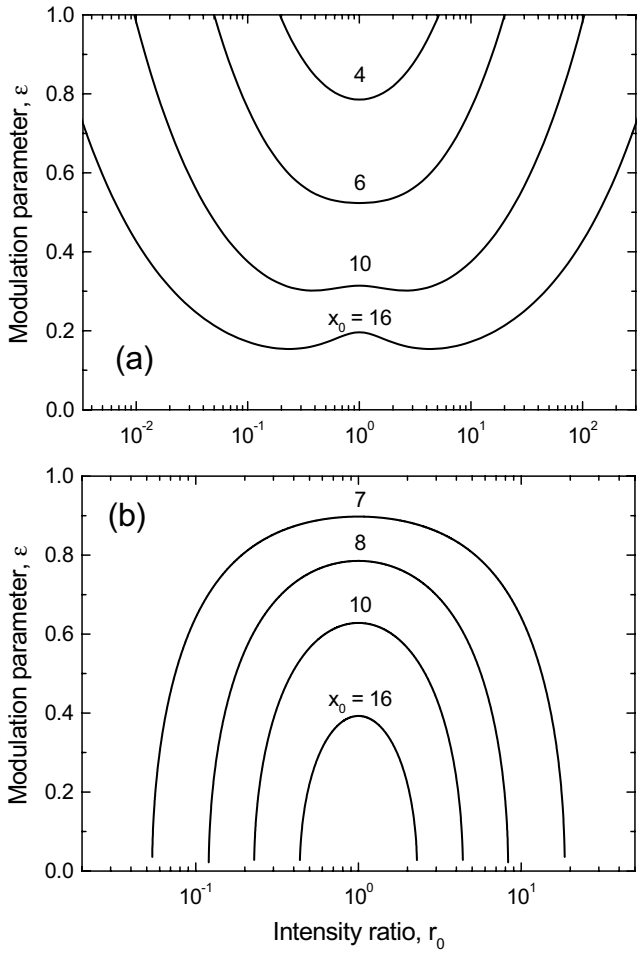

Fig. 2. Dependence $\varepsilon(r_0)$ for different values of the crystal thickness x_0; cases (a) and (b) refer to the $+\pi/2$ and $-\pi/2$ feedback conditions, respectively

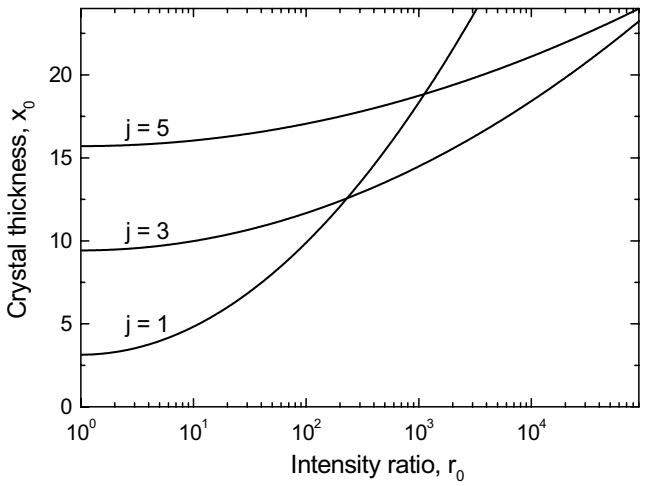

Fig. 3. Threshold dependences $x_0(|\lg\ r_0|)$ for the $+\pi/2$ feedback condition and $j = 1,\ 3,\ 5$

B. Average Characteristics of the Periodic States

Relations (12), (13) include two feedback-controlled parameters, Ω and ε. Thus, the condition $\eta = 1$ (i. e., $R_F(x_0) = 0$ and $S_F(x_0) = 1$) or $\eta = 0$ (i. e., $R_F(x_0) = 1$ and $S_F(x_0) = 0$) can be fulfilled within the first order of perturbation theory.

It is easy to find out from Eq. (12) that $\eta = 1$ when

$$x_0 = \frac{\pi^2 j^2 + L^2}{g\pi j}, \quad \Omega = -\frac{L}{\pi j}\,, \tag{17}$$

where $L = \ln[(g - W_0)/(g + W_0)]$, and $j = 1,\ 3,\ \ldots$ is a positive odd number. Since $g = g(\varepsilon,\ W_0)$, the first relation gives a sequence of branches $\varepsilon_j(x_0,\ W_0)$, while the second one yields the frequency detuning as a function of x_0 and W_0 for the j-branch. One can see that Ω and ε are even and odd functions of W_0, respectively. Fig. 2,a shows the dependence $\varepsilon(r_0)$ for the branch $j = 1$ and several representative values of x_0. The actual values of $|\Omega|$ do not exceed 1.5.

Since $\varepsilon \le 1$, the values of x_0 and $|\ln\ r_0|$ are restricted from below and above, respectively. To determine the region of parameters $x_0,\ r_0$ where the periodic states with $\eta = 1$ are attainable, we set $\varepsilon = 1$ in Eqs. (16), (17). This brings us to the equality

$$x_0 = \pi j + \frac{\ln^2 r_0}{\pi j} \tag{18}$$

which describes the boundary of the region in question. The minimum possible thickness is $x_0^{\min} = \pi$, it corresponds to $r_0 = 1$ for the branch $j = 1$. For this branch $|\ln r_0|_{\ max} = \sqrt{\pi(x_0 - \pi)}$; the allowed range of r_0 grows quickly with increasing x_0. Fig. 3 shows the dependences $x_0(r_0)$ for $j = 1,\ 3,\ 5$. Within a fairly wide range of parameters, $\pi \le x_0 \lesssim 12.5$ and $|\ln r_0| \lesssim 2$, the branch $j = 1$ is the lowest. It is of our main interest.

The average characteristics of the periodic states with $\eta = 0$ (fully transparent grating) meet the condition $\bar{S}_F(x_0) = 0$. Using Eq. (13), we represent it in the form $\gamma' = 0$, $\gamma'' x_0 = -\pi j'$ with $j' = 2,\ 4,\ \ldots$. This is equivalent to the equalities

$$\varepsilon^2 = \frac{(\pi j'/x_0)^2 - W_0^2}{1 - W_0^2}\,, \quad \Omega = 0. \tag{19}$$

The minimum thickness $x_0^{\min} = 2\pi$ corresponds here to $j' = 2$ and $W_0 = 0$ ($r_0 = 1$); it is two times larger than the previous one. The function $\varepsilon(\lg r_0)$ for

$j' = 2$ and several representative values of x_0 is shown in Fig. 2,*b*. It is even and decreasing with x_0 and $|\lg\ r_0|$. The allowed range of r_0 decreases thus with increasing x_0. By setting $\varepsilon = 0$ we obtain the following inequality for the range of allowed parameters: $|W_0| \leq 2\pi/x_0$.

C. Fast Components of the Amplitudes

In the next order of perturbation theory, the fast components of the amplitudes can be found. For the fast component of the grating amplitude, Eqs. (3), (8) — (10) yield the the following dynamic equation:

$$\tilde{E}_t = |R_0 S_0| \left[(\bar{R}_F^2 - \bar{S}_F^{*2})(\cos\varphi_p - \varepsilon) - \right.$$
$$\left. - i \sin\varphi_p \, (\bar{R}_F^2 + \bar{S}_F^{*2})\right] . \qquad (20)$$

Since the time and coordinate dependences on the right-hand side of Eq. (20) are separated, this equation can be integrated easily. The result of this integration is

$$\tilde{E} = |R_0 S_0| \left[(\bar{R}_F^2 - \bar{S}_F^{*2})u - i(\bar{R}_F^2 + \bar{S}_F^{*2})v\right] . \qquad (21)$$

The periodic functions of time $u(t)$ and $v(t)$ are defined by the equations:

$$\dot{u} = \cos\varphi_p - \varepsilon, \quad \dot{v} = \sin\varphi_p , \qquad (22)$$

where the dots denote again the ordinary time derivatives.

For the fast components of the fundamental amplitudes, Eqs. (1), (2) give a linear system of ordinary differential equations. It can be solved by the method of variation of constants. The final result can be presented in the form

$$\tilde{R}_F(x,t) = A(x,t)\bar{R}_F(x) - B(x,t)\bar{S}_F^*(x),$$
$$\tilde{S}_F(x,t) = A(x,t)\bar{S}_F(x) + B(x,t)\bar{R}_F^*(x), \qquad (23)$$

where the functions $A(x,t)$ and $B(x,t)$ are given by

$$A(x,t) = 2i \int_0^x \mathrm{Re}[\tilde{E}(x',t)\, \bar{R}_F^*(x')\, \bar{S}_F(x')]\, dx',$$
$$B(x,t) = i \int_0^x [\tilde{E}^*(x',t)\, \bar{R}_F^2(x') -$$
$$- \tilde{E}(x,t)\, \bar{S}_F^2(x')]\, dx'. \qquad (24)$$

To make the description of the periodic states self-consistent, we have to satisfy the feedback condition (6). Using Eqs. (5) and (7), we rewrite this condition as

$$\dot{\varphi_s} = \mp\, t_f^{-1}\, \Re[R_0 S_0^* R_F(x_0) S_F(x_0) \exp(-i\Omega t - i\varphi_p)]. \qquad (25)$$

For the periodic states controlled by the $+\pi/2$ (or $-\pi/2$) feedback, the value $\bar{R}_F(x_0)$ (or $\bar{S}_F(x_0)$) equals zero. Using this fact and also Eqs. (8, 9, 23), we obtain that

$$R_F(x_0) S_F(x_0) \exp(-i\Omega t) \simeq \mp B(x_0, t) . \qquad (26)$$

The function $B(x_0, t)$ is determined by Eq. (24). By making use of Eq. (21,) we obtain lastly

$$|R_0 S_0| B(x_0, t) = -c_+ v + i c_- u , \qquad (27)$$

for the product entering Eq. (25), where the constants $c_\pm$ are determined by

$$c_\pm = |R_0 S_0|^2 \int_0^{x_0} (1 \pm 2\bar{R}_F^2 \bar{S}_F^2 - 2|\bar{R}_F \bar{S}_F|^2)\, dx. \qquad (28)$$

The amplitudes $\bar{R}_F(x)$ and $\bar{S}_F(x)$ entering this relation correspond to the states with $\eta = 1$ or 0. The constants $c_\pm$ can be calculated for any x_0, r_0, and the branch j. For example, in the case of equal input intensities, we have $c_+ = x_0/8$ and $c_- = x_0/4$. It is important that $c_\pm$ are real. This property follows from the fact that the real and imaginary parts of the function $\bar{R}_F(x)\bar{S}_F(x)$ possess different parity signs with respect to the crystal center.

By substituting Eqs. (26), (27) into Eq. (25), we obtain finally the equation for the input phase φ_p:

$$t_f\, \dot{\varphi_p} = c_-\, u\, \sin\varphi_p - c_+\, v\, \cos\varphi_p. \qquad (29)$$

Its form does not depend on the feedback sign. It is evident that scaling of the constants $c_\pm$ is equivalent to a renormalization of the response time t_f. The ratio c_+/c_- determines thus the character of the periodic state. In the case $\eta \simeq 1$, this ratio grows from 0.5 to $\approx$ 0.7 with increasing x_0 or $|\lg r_0|$. In the case $\eta \simeq 0$, it can reach the value of 1 – 1.2.

One can see that the set of three ordinary differential equations, Eqs. (22) and Eq. (29), describes the periodic states. This system is strongly nonlinear; its integration cannot be performed analytically. We study the periodic solutions using the standard numerical routines of Matlab. This allows us to avoid direct time-consuming simulations of the basic partial differential equations and to reveal a variety of allowed periodic states.

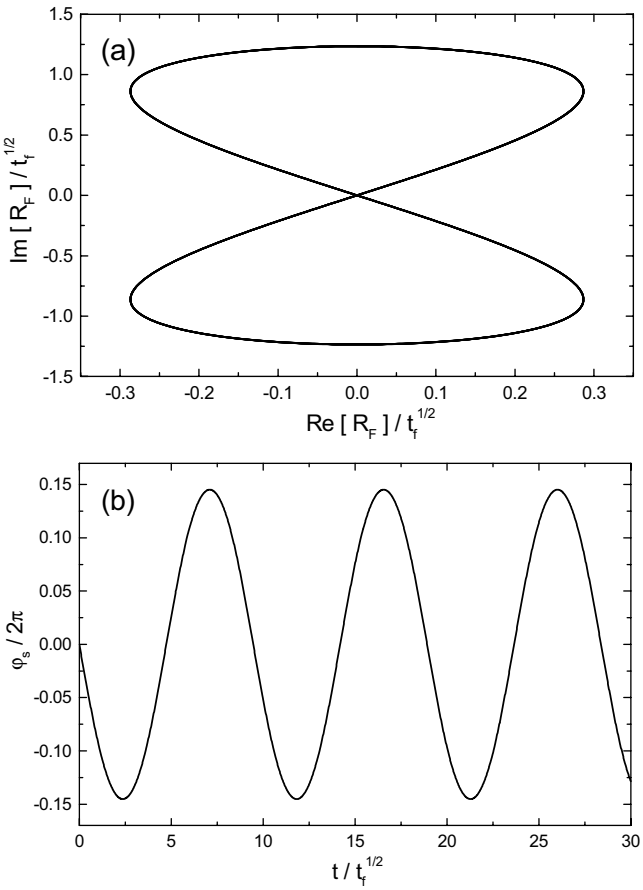

Fig. 4. a — closed trajectory $R_F(x_0, t)$ for the periodic state with $N = 0$, $r_0 = 1$, and $x_0 = \pi/0.8 \simeq 3.9$ relevant to the $+\pi/2$ feedback. b — the corresponding time dependence of the input phase φ_s

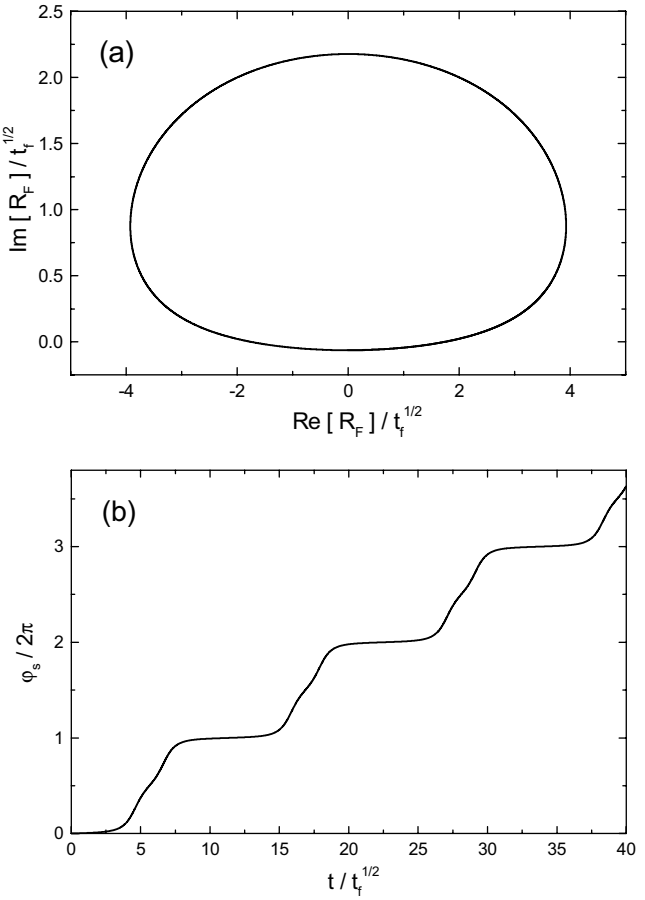

Fig. 5. Characteristics of the periodic state with $N = 1$ for $r_0 = 1$ and $x_0 = \pi/0.6 \simeq 5.24$; subfigures ($a$) and ($b$) show the closed trajectory and the phase dependence $\varphi_s(t)$

3. Characteristics of the Periodic States

The period of fast oscillations T and the maximum deviation of the diffraction efficiency from its extreme value $\delta\eta_{\max}$ depend on the feedback loop response time t_f. The set of equations (22), (29) allows one to obtain these dependences. Normalizing the time t and the functions u, v by $\sqrt{t_f}$, one can exclude the parameter t_f from the dynamic equations. Thus, the following scaling relations hold true:

$$T \propto \sqrt{t_f}, \quad \delta\eta_{\max} \propto t_f \ . \tag{30}$$

They are in full agreement with the results of direct simulations [12, 13].

In a T-periodic state, the fast component of the input phase obeys the relation $\varphi_p(t + T) - \varphi_p(t) = 2\pi N$, where N is an integer. It is convenient to classify the periodic solutions according to this number. If a set $\varphi_p(t)$, $u(t)$, $v(t)$ represents such a solution, then the functions $-\varphi_p(t)$, $u(t)$, $-v(t)$ give a solution as well. Therefore, the states with the numbers N and $-N$ are conjugated and we can restrict ourselves only to $N \geq 0$.

In the case of $+\pi/2$ feedback, we have $\bar{S}_F(x_0) \simeq -i$ and $R_F(x_0, t) \simeq (c_- u + ic_+ v)/|R_0 S_0|$. The closed trajectory on the complex plane given by the function $R_F(x_0, t)$ serves well for a graphic representation of the corresponding periodic state. The square of the distance of a trajectory from the 0 point gives the deviation $\delta\eta(t)$. For the $-\pi/2$ feedback, the closed trajectory given by $S_F(x_0, t) \simeq (-ic_- u + c_+ v)/|R_0 S_0|$ has to be used instead.

Now we proceed to particular results. One of the most important questions to answer is what happens with the periodic states with varying super-criticality (i.e., the distance to the threshold). Consider, for

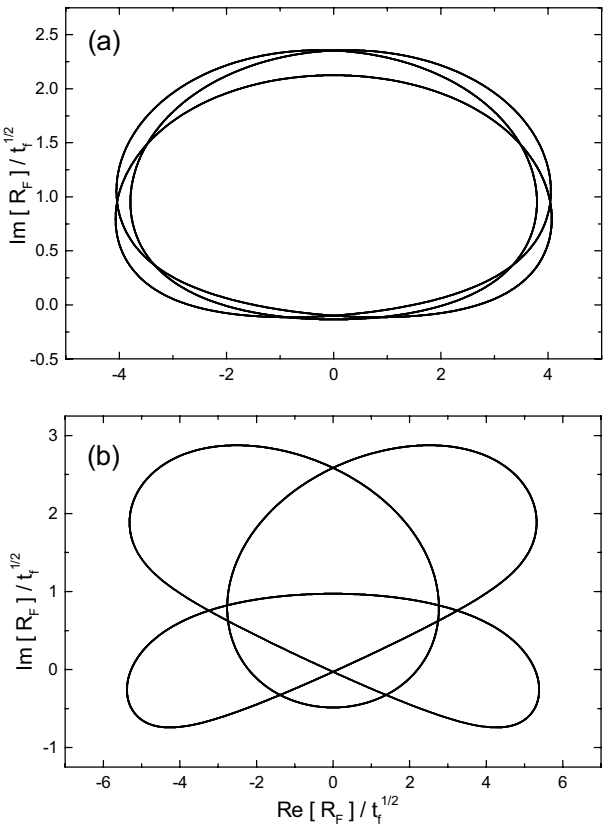

Fig. 6. Closed trajectories for the periodic state with $N = 3$; cases (a) and (b) correspond to $x_0 = \pi/0.54 \simeq 5.82$ and $x_0 = 2\pi$, respectively

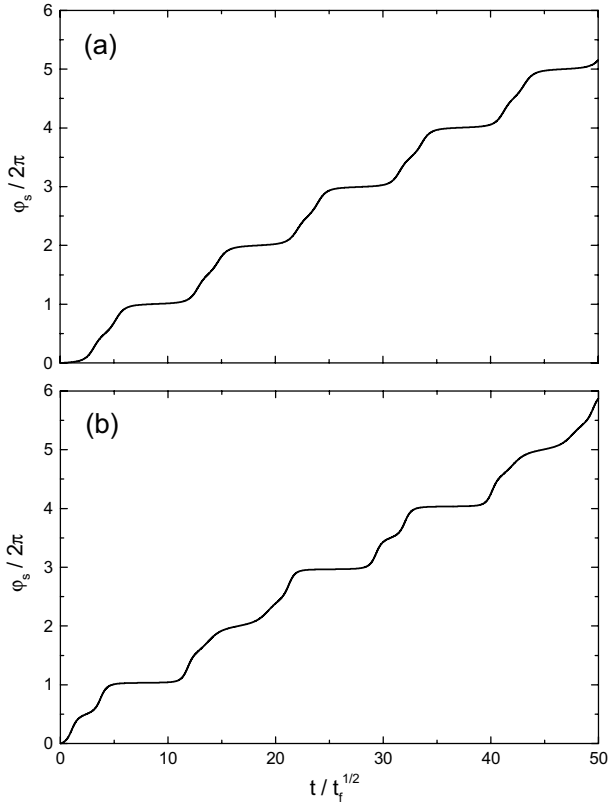

Fig. 7. Dependence $\varphi_s(t)$ for the periodic state with $N = 3$; cases (a) and (b) correspond to Figs. 6,a and b, respectively

simplicity, the case $\eta \simeq 1$, $r_0 = 1$ when the difference $x_0 - \pi = \pi(\varepsilon^{-1} - 1)$ serves as the natural parameter of super-criticality. Our simulations show that, within the interval $\pi < x_0 \simeq 4.2$, where ε is changing from 1 to $\simeq 0.74$, the only possible periodic state is the state with $N = 0$. Fig. 4,a and 4,b show the relevant closed trajectory and the input phase behavior for $\varepsilon = 0.8$ ($x_0 = \pi/\varepsilon \simeq 3.9$). The period of oscillations is $T_0 \simeq 5.25\sqrt{t_f}$. When approaching the threshold ($\varepsilon \to 1$) the size of the attractor and the amplitude of phase oscillations tend to zero, whereas the period T remains almost unchanged.

In the region $4.2 \lesssim x_0 \lesssim 5.7$ ($0.74 \gtrsim \varepsilon \gtrsim 0.54$), in addition to the state with $N = 0$, the periodic state with $N = 1$ becomes achievable. The corresponding bagel-like trajectory and phase dependence are shown in Fig. 5,a,b for $\varepsilon = 0.6$ ($x_0 \simeq 5.24$). Only one revolution around zero occurs during the period of $T_1 \simeq 9\sqrt{t_f}$, compare with Fig. 4,a. The phase dependence $\varphi_s(t)$ is distinguished by step-like behavior; during each step, the phase is increasing by 2π. The size of the attractor and the period T_1 are noticeably larger as compared to the previous case. No dramatic changes of the state with $N = 1$ occur when the thickness x_0 approaches from above the value $\simeq 4.2$. With a further decreasing of x_0, it is not possible to find a closed trajectory with $N = 1$ (i.e., the periodic state loses its stability).

For $x_0 \gtrsim 5.7$ ($\varepsilon \lesssim 0.54$), the periodic state with $N = 3$ becomes possible. It appears via the period-tripling bifurcation of the state with $N = 1$. The corresponding closed trajectory consists of three lobes, see Fig. 6,a,b. Each of them is initially (for $x_0 - 5.7 \ll 1$) very close to the bagel-like orbit of the state with $N = 1$, compare with Fig. 5,a. However, the trajectory returns to a starting point only after three revolutions around zero and the oscillation period $T_3(x_0) \simeq 3T_1(x_0)$. With increasing x_0, the difference between the states with $N = 3$ and 1 becomes more and more pronounced. The graph of $\varphi_s(t)$ includes three substeps during a period of T_3, the difference between them is increasing with x_0, see Fig. 7,a,b.

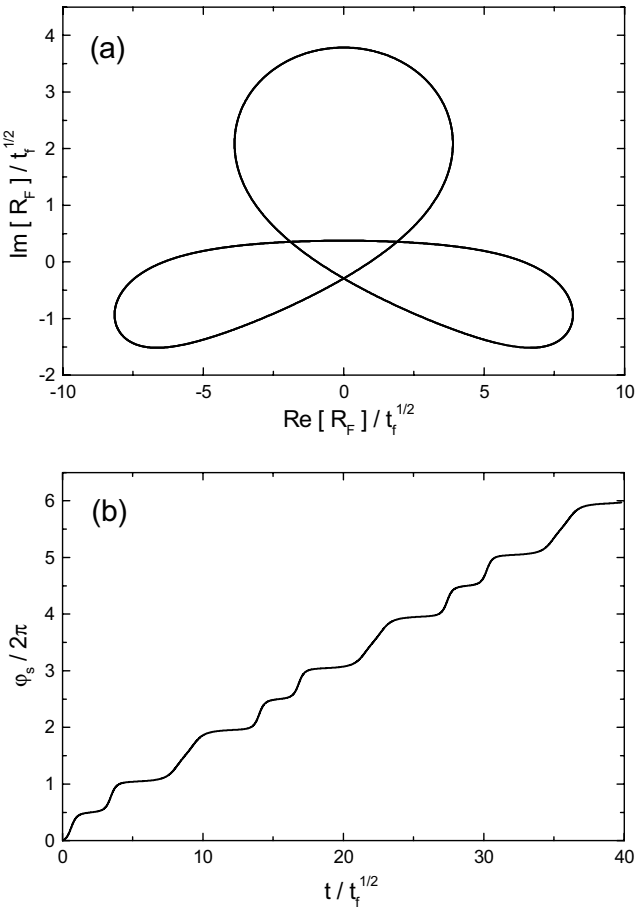

Fig. 8. Characteristics of the periodic state with $N = 2$ for $x_0 = 10$; subfigures (a) and (b) show the trajectory and the input phase behavior

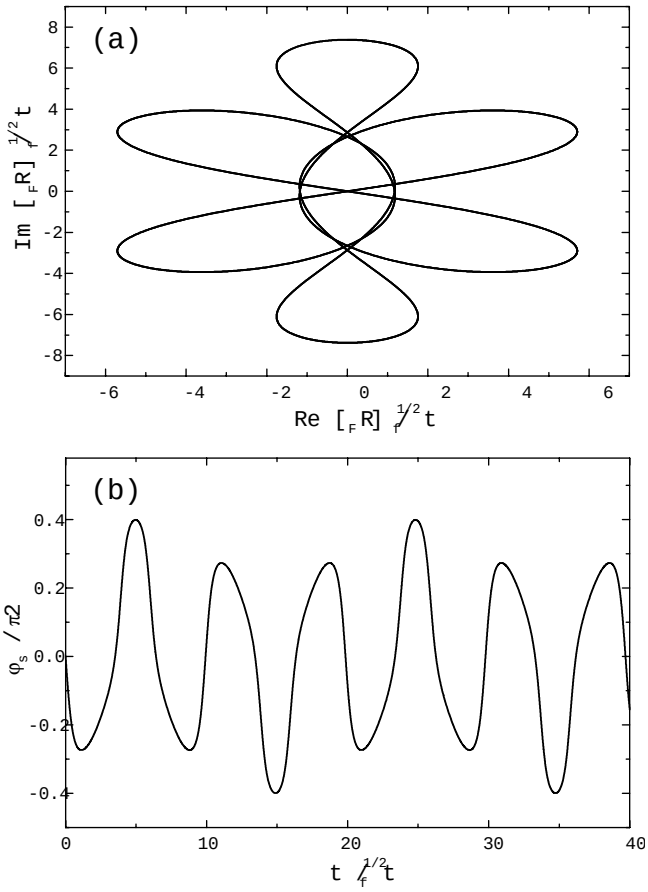

Fig. 9. Closed trajectory (a) and the phase dependence (b) for the periodic state with $N = 0$ at $x_0 = \pi/0.2 \simeq 15.7$

The periodic state with $N = 2$ becomes possible only for $x_0 \gtrsim 6.73$ ($\varepsilon \lesssim 0.467$) via a doubling-period bifurcation of the state with $N = 1$ The corresponding trajectory and the input phase behavior at $x_0 = 10$ ($\varepsilon = 0.314$) are illustrated by Fig. 8,a,b. Two noticeably different substeps occur during a period of $T_2 \simeq 9\sqrt{t_f}$.

We see that the number of possible periodic states is growing quickly with increasing the super-criticality parameter $x_0 - \pi$. It is worth mentioning that the complexity of the situation may increase with x_0 not only because of increasing N, but also because of increasing the number of the states with the same N. This is illustrated by Fig. 9 that shows the trajectory and the dependence $\varphi_s(t)$ relevant to the periodic state with $N = 0$ at $\varepsilon = 0.2$ ($x_0 \simeq 15.7$). The state with $N = 0$, which is similar to that shown in Fig. 4, is also available for the same x_0.

We have considered above what happens with the periodic states when we recede from the threshold through increasing x_0 at $r_0 = 1$. Qualitatively the same behavior takes place when we fix the thickness x_0 and decrease the parameter $|\ln r_0|$ from the threshold value $\sqrt{\pi(x_0 - \pi)}$ to 0. This is greatly because of the fact that the ratio c_+/c_- does not depend strongly on x_0 and r_0.

Summary

We have developed a new analytical method for the description of feedback-controlled periodic states in photorefractive crystals. It makes use of the symmetry properties of the coupled-wave equations and the property of quickness of the feedback loop. To the best of our knowledge, this method has no analogs among the known nonlinear systems.

A number of new theoretical results is obtained with the new method: The spatial structure of the index gratings relevant to the states with $\eta = 1$ and 0 is described. The scaling relations for the oscillation period T and the oscillation amplitude $\delta\eta_{\max}$ are derived. It is described in detail what happens with the periodic states as we increase the super-criticality; this includes the number of the states available, the corresponding periods and the shape of feedback-controlled phase oscillations. A close connection between the characteristics of the states with $\eta = 1$ and 0 is established.

The found analytical results comply well with the known results of direct simulations [12]. Furthermore, they supplement essentially the numerical results and elucidate greatly the nature and range of variation of the periodic nonlinear states.

It is important that the periodic states are not unique in the general case. Several qualitatively different states can be available with the same input and material parameters. Which of them should be realized depends, probably, on the choice of the initial state and the excitation mode. On the other hand, the multiplicity of the periodic states makes important the problem of their stability. This problem is open for the subsequent studies.

Financial support from the Russian Foundation for Fundamental Studies (Grant 03-02-16083) is gratefully acknowledged.

1. *Günter P., Huignard G.P.* Topics in Applied Physics. — Vol. 61: Photorefractive Materials and Their Applications. — Berlin: Springer, 1989.
2. *Petrov M.P., Stepanov S.I., Khomenko A.V.* Photorefractive Crystals in Coherent Optical Systems. — Berlin: Springer, 1991.
3. *Solymar L., Webb D.J., Grunnet-Jepsen A.* The Physics and Applications of Photorefractive Materials. — Oxford: Clarendon Press, 1996.
4. *Stepanov S.*// Repts. Prog. Phys.— 1994.— **57**.— P.39.
5. *Cronin-Golomb M., Fischer B., White J.O., Yariv A.*// IEEE J. Quant. Electron.— 1984 **QE-20**.— P.12.
6. *Odoulov S.G., Soskin M.S., Khyzhniak A.I.*// Dynamic Grating Lasers. — London: Harword, 1991.
7. *Sturman B., Odoulov S., Goul'kov M.*// Phys. Repts.— 1996.— **275**.— P.197.
8. *Freschi A., Frejlich J.* //J. Opt. Soc. Amer. B.— 1994.— **11**.— P.1837.
9. *Garcia P.M., Buse K., Kip D., Frejlich J.*// Opt. Communs.— 1995.— **117**.— P.35.
10. *Garcia P.M., Freschi A.A., Frejlich J., Krätzig E.*// Appl. Phys. B.— 1996.— **63**.— P.207.
11. *Kamenov V.P., Ringhofer K.H., Sturman B.I., Frejlich J.*// Phys. Rev. A.— 1997.— **56**.— P.R2541.
12. *Podivilov E.V., Sturman B.I., Odoulov S.G. et al.*//Ibid.— 2001.— **63**.— P.053805.
13. *Podivilov E.V., Sturman B.I., Odoulov S.G. et al.*// Opt. Communs.— 2001.— **192**.— P.399.
14. *Ringhofer K.H., Kamenov V.P., Sturman B. et al.*//Phys. Rev. E.— 1999.— **61**.— P.2029.

АНАЛІТИЧНА ТЕОРІЯ ПЕРІОДИЧНИХ СТАНІВ У ФОТОРЕФРАКТИВНИХ КРИСТАЛАХ ІЗ ЗВОРОТНИМ ЗВ'ЯЗКОМ

Е.В. Подівілов, Б.І. Стурман, М. Горкунов

Р е з ю м е

Застосування деяких схем зворотного зв'язку в фоторефрактивних оптичних схемах дозволяє реалізувати періодичні стани (атрактори) з надзвичайно високою або низькою дифракційною ефективністю. Цей нелінійний феномен було вивчено експериментально та чисельно. Ми запропонували та розвинули аналітичний метод для аналізу періодичних станів, використовуючи симетрійні рівняння зв'язаних хвиль і швидкий відгук кільця зворотного зв'язку. Детально описано різні періодичні стани. А саме зони їх існування, період та амплітуду осциляцій вимірюваних вихідних параметрів, а також форми сильних неперіодичних фазових модуляцій вхідного променя.